

# Determining the Generator Potier Reactance for Relevant (Reactive) Loads

Miloje Kostić

Electrical Engineering Institute Nikola Tesla, University of Belgrade, Serbia  
E-mail: mkostic@ieent.org

**Abstract:** Following results of an investigation the author comes to the conclusion: that the Potier reactance values depend almost solely on the turbogenerator(s) reactive currents ( $i_{aQ} = i_{an} \sin \varphi$ ) for a given voltage value. This new rule is after being proven by a general qualitative analysis, and his thesis is then checked for rated values of the active and reactive power, for an example of a GTHW 360 (360 MW) turbogenerator. Potier reactance  $x_p$  is determined by the open-circuit saturation characteristics and data from the zero-power factor at the rated voltage ( $i_a = i_{a,90} \cos \varphi = 0$ ,  $U = U_n$ ). The procedures used to determine the Potier reactance ( $x_p$  or  $x_{p,n}$ ) are performed by a computer with the open-circuit saturation curves  $i_{f0}(e_0)$  expressed analytically. The author proposes the IEC 34-4 standard in the part on the determination of the Potier reactance. It is proposed that it is determined for the excitation current corresponding to the rated voltage and armature current value  $i_{a,90} = i_{an} \sin \varphi_n$ , at the zero-power factor (overexcitation), and for some characteristic values is needed for the construction of the turbogenerator capability curve (P-Q curve).

**Keywords:** Reactive power, synchronous generator, turbogenerator, rotor saturation, leakage reactance, Potier reactance, excitation current, reactive load test, capability curves.

## Določitev Potierjeve reaktance za reaktivna bremena

V članku analiziramo odvisnost Potierjeve reaktance od reaktivnega toka ( $i_{aQ} = i_{an} \sin \varphi$ ) v generatorju za dano napetost. Podana teoretična analiza je eksperimentalno potrjena z generatorjem GTHW 360 (360 MW). Potierjeva reaktanca  $x_p$  je določena s karakteristiko odprtih sponk in faktorja moči pri različnih napetostih ( $i_a = i_{a,90} \cos \varphi = 0$ ,  $U = U_n$ ). Na podlagi dobljenih rezultatov predlagamo spremembe v standardu IEC 34-4 v delu, ki se nanaša na določanje Potierjeve reaktance.

## 1 INTRODUCTION

The excitation (field) current required for operating a synchronous generator (SG) at a rated steady-state active power, power factor, and voltage, is an important factor in the thermal design of a machine. To determine the excitation current under specified load conditions, the Potier reactance  $X_p$  (or leakage reactance  $X_\ell$ ), unsaturated direct-axis and quadrature-axis reactance,  $X_{du}$  and  $X_{qu}$ , armature resistance  $R_a$ , and the open-circuit saturation curve  $e_0(i_f)$  are needed. Methods for determining the Potier reactance are especially important since they take into account the rotor additional saturation due to field of the excitation winding on load in the overexcited regime and  $X_p$  is greater than the real value of the armature leakage reactance ( $X_p > X_\ell$ ).

An accurate determination of the armature leakage reactance of synchronous machines is essential for the analysis of these machines [1–5]. Although numerical

techniques for calculating this reactance have been suggested in the literature, there has been no practical method to accurately determine its value experimentally, owing to the fact that it is difficult to directly measure the armature leakage flux [6, 7]. For experimental machines, search coils inserted in the air gaps of the machines have been used to detect this leakage flux [5]. In general, the armature leakage reactance is usually approximated by the Potier reactance measured at the rated terminal voltage [8, 9]. However, the values of the Potier reactance of synchronous machines measured at the rated terminal voltage can be much larger than those of the armature leakage reactances [1]. Following the author's investigation [11], it is confirmed that the discrepancies between the values of the Potier reactance and the armature leakage reactance of four synchronous machines can be as high as 50%. Recent investigations of experimental synchronous machines have also resulted in the same observation [12]. Instead measuring the Potier reactance at the rated terminal voltage, March and Cary propose that the measuring of the Potier reactance at a higher value of the terminal voltage could result in a more accurate value of the armature leakage reactance. However, application of this method is difficult since the machine under test may not be able to withstand the high values of the field current at which the armature leakage reactance is well approximated by the Potier reactance. In order to obtain more accurate values of the armature leakage reactance without any risk to the machines under test, an alternative method is proposed [1].

However, it is more important to establish the Potier reactance real values than the accurate values of the armature leakage reactance, due to the following facts:

1. Leakage reactance  $X_l$  is almost independent of the magnetic circuit saturation and is therefore assumed to be constant.
2. The saturation curve of the synchronous generator under its loaded states is assumed to be the same as the open-circuit characteristic. According to this assumption, the field leakage flux is assumed to have the same effect under load as under no-load state. Any error introduced by the using the open-circuit characteristic is empirically compensated for by using the Potier reactance ( $X_p > X_l$ ).
3. The field MMF, equivalent to the armature MMF, and corresponding field current component  $I_{af}$  can be found from the unsaturated armature reactance  $X_a$ .
4. The air gap is assumed to be uniform so that the direct-axis synchronous reactance  $X_d$  is equal to the quadrature axis synchronous reactance  $X_q$ . For nonsalient-pole synchronous machines (turbogenerator), in practice this means  $X_d = X_q$ . The unsaturated direct-axis synchronous reactance is calculated by equation  $X_{du} = X_a + X_l$ .

In numerous investigations [1, 6, 12], it is shown that the Potier reactance values depend on the terminal voltage values. Results of the author's investigations [10, 11] also show that the Potier reactance essentially depends on the reactive load values for a given voltage value. In this paper, changes and additions to the IEC 34-4/2008 standard are proposed in the part for the determining the Potier reactance [9].

## 2 THE POTIER REACTANCE DEPENDENCE ON REACTIVE LOADS

An equivalent reactance ( $X_p$ ), used instead of the armature leakage reactance to calculate the excitation in the on load state, is determined by means of the Potier methods. They take into account the rotor additional saturation due to the field of the excitation winding on the load in the overexcited regime, and  $X_p$  is greater than the real value of the armature leakage reactance. In a rated voltage tests, the Potier reactance  $X_p$  may be larger than the actual leakage reactance by as much as 20 to 30% [1, 4, 13]. The author's investigation [11, 12] confirms that the discrepancies between the values of the Potier reactance and the armature leakage reactance of four synchronous machines can be as high as 50%. Namely the additional leakage flux of the field winding on load, in the overexcited regime leads to a further increase in the Potier reactance  $X_p$ . Thus, changes and additions are proposed to the IEC 34-4/2008 standard, "Rotation Electrical Machines, Part 4: Methods for determining synchronous machine quantities from tests" in the part on the determination of the Potier reactance [9]. It is proposed that  $X_p$  is determined by the excitation current corresponding to the rated voltage and armature current value  $i_{a,90} = i_{an} \cdot \sin\varphi_n$ , at the zero-power factor

(overexcitation), and for some characteristic values that would be convenient for the construction of the turbogenerator capability curve, i.e. the  $P-Q$  curve. Namely based on investigations [10, 14], the author comes to a new conclusion: that in practice the Potier reactance values depend solely on the turbogenerator reactive currents ( $i_{aQ} = i_{an} \cdot \sin\varphi$ ) for the given voltage values.

The author's thesis proven by qualitative analysis and the Potier reactance values determined by the Potier method. A standard graphical method is used determine the Potier reactance [9] from the following data:

- a) the no-load saturation characteristic and sustained three-phase short-circuit characteristic, and
- b) the excitation current corresponding to the rated voltage and rated armature current at the zero power-factor (overexcitation).

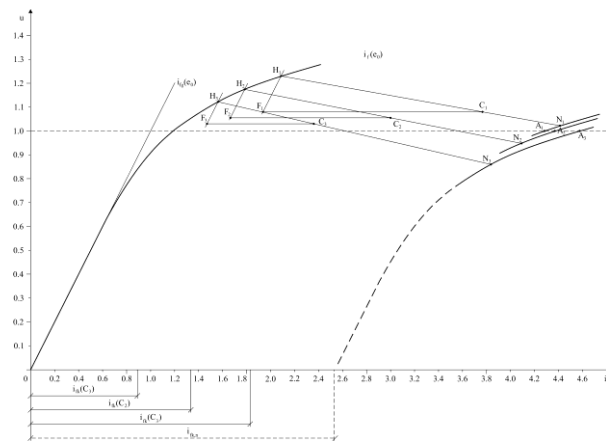


Figure 1. Experimental points  $C_1$ ,  $C_2$  and  $C_3$  from reactive load tests with armature currents  $i_{a(C1)} > i_{a(C2)} > i_{a(C3)}$ , and corresponding points  $A_1$ ,  $A_2$  and  $A_3$  on the reactive load curves which correspond to the rated voltage

If, during the overexcitation test at the zero power-factor, the voltage and current differ from the rated value by no more than  $\pm 0.15$  per unit, a graphical method is used to determine of the excitation current corresponding to the rated voltage and current [9]. In contrast, the author proposes [11, 12] the overexcitation test at the zero power-factor to be performed for at least three values of armature current ( $I_a$ ) and corresponding generator voltages, i.e.

- $I_{a1} = I_{a,max} > I_{aN} \cdot \sin\varphi_N$  (i.e.  $Q_{G1} = Q_{Gmax} > Q_{GN}$ ), which corresponds to excitation rated current ( $I_f = I_{fn}$ ) and  $U_{G1} = U_G$  at  $Q_{G1} = Q_{Gmax} > Q_{GN}$  (approximately: point  $C_1$ , Figure 1);
- $I_{a2} = I_{aN} \cdot \sin\varphi_N$  (i.e.  $Q_{G2} = Q_{GN}$ ) and  $U_{G2} = U_G$  at  $Q_2 = Q_N$  (approximately: point  $C_3$ , Figure 1); and
- $I_{a3} \approx (I_{a1} + I_{a2})/2$ , i.e.  $Q_{G3} \approx (Q_{Gmax} + Q_{GN})/2$  and  $U_{G3} = U_G$ .

For three experimental armature currents (Fig. 1),  $i_{a1(C1)} > i_{a2(C2)} > i_{a3(C3)}$ , the following different reduced armature current values (for rated voltage) are obtained:

- $i_{a(C1)} \rightarrow i_{a(A1)}$ ;  $i_{a(C2)} \rightarrow i_{a(A2)}$  and  $i_{a(C3)} \rightarrow i_{a(A3)}$ ;

- with  $i_{a(A1)} < i_{a(A2)} < i_{a(A3)}$ .

Corresponding and different values of Potier reactance are obtained (Fig. 2), as shown follow:

$$X_{P(A1)} < X_{P(A2)} < X_{P(A3)}, \text{ for } i_{a(C1)} > i_{a(C2)} > i_{a(C3)} \quad (1)$$

### 3 A NEW RULE FOR THE POTIER REACTANCE DETERMINATION AND THE ANALYSIS OF ITS DEPENDENCE ON REACTIVE LOADS

Based on the results of the investigations [101, 11, 14], the author comes to the conclusion: that the value of the Potier reactance, for a given voltage value, depends almost exclusively on the reactive load values ( $i_{aQ} = i_a \cdot \sin\varphi$ ). This new rule is proven: a) first, by a qualitative analysis, and b) then by checking made on an example of a GTHW 360 (360 MW) turbogenerator for the relevant values of the regime of the active and reactive loads [12, 15]. Potier reactance  $x_p$  is determined by open-circuit saturation and the zero-power factor rated current ( $i_{a,90} = i_n, \cos\varphi = 0, U = U_n$ ). The procedures for determining the Potier reactance ( $x_p$  or  $x_{p,n}$ ) are performed by a computer (Excel program), with the open-circuit saturation curve  $i_{f0}(e_0)$  expressed analytically. With this, the procedure is simplified and more precise.

In addition to the graphical procedure for determination of the Potier reactance ( $x_{p,n}$ ) for the rated generator regime ( $u = u_n, i = i_n, \varphi = \varphi_n$ ), Fig.3, shows also graphic determination of the Potier reactance value ( $x_{p,90n}$ ) for the reactive load regime with the rated load ( $u = u_n, i_{90} = i_n, \varphi = 90^\circ$ ). The procedure for to the determine the Potier reactance ( $x_{p,90n}$ ) has been runs in the order marked by numbers 7 and 8 and is identical to the procedure applied to determine the reactance value ( $x_{p,n}$ ). The reactance values  $x_{p,n}$  and  $x_{p,90n}$  are set by means of the procedure illustrated in Fig. 3.

The magnetization curve of the machine under load,  $i_{fl}(e_l)$ , is constructed and given in Fig. 3. The Potier reactance value for the rated regime ( $x_{p,n}$ ) exceeds the value for the reactive load regime with rated current ( $x_{p,n,90}$ ), i.e.  $x_{p,n} > x_{p,90n}$  (Fig. 3). The reason for this are which the electromotive forces behind the Potier reactance ( $e_p$ ) which have a larger value in the reactive load regime with rated current ( $u = u_n, i_{90} = i_n, \varphi = 90^\circ$ ), i.e.  $e_{p90} = 0F > 0C = e_{p,n,90}$  (Fig. 3), so that in such a load regime the turbogenerator magnetic circuit saturation is larger and the corresponding reactances are therefore smaller. For a certain turbogenerator [15], the Potier reactance value for the rated region ( $x_{p,n}$ ) is by 20% larger.

The fact that the Potier reactance value for a given power system voltage value depends almost exclusively on the reactive current load value ( $i_{aQ} = i_a \cdot \sin\varphi$ ) is shown in Fig. 4. Besides the Potier reactance value ( $x_{p,n}$ ) for the rated generator region ( $u = u_n, i = i_n$  and  $\varphi = \varphi_n$ ) ( $i_{an}$ ), Fig. 4 includes also a graphic determination of the Potier reactance value ( $x_{p,n,90}$ ) for the reactive load regime  $i = i_{a90} = i_{an} \cdot \sin\varphi_n$ . The procedure to determine the Potier reactance ( $x_{p,n,90}$ ) is runs in the order marked

by numbers 7 and 8 and is identical to the procedure for determining value  $x_{p,n}$ . The procedure described was conducted for the same turbogenerator as the one in Fig.3. Since the voltage value ( $x_{p,n} i_{an} \sin\varphi_n = x_{p,90n} (i_{an} \sin\varphi_n)$ ) (Fig. 4), the Potier reactance value for the rated regime ( $x_{p,n}$ ) is approximately equal to the value ( $x_{p,90n}$ ), for the reactive load regime with  $i_{90} = i_{an} \cdot \sin\varphi_n$  ( $u = u_n, i_{90} = i_{an} \cdot \sin\varphi_n$  and  $\varphi = 90^\circ$ ), i.e.:

$$x_{p,n} \approx x_{p,90n}, \text{ for } i_{a90} = i_{an} \sin\varphi_n \quad (2)$$

Based on of the equivalence (2) and illustrations in Fig. 4, a general equivalence can be written as given below:

$$x_p \approx x_{p,90}, \text{ for } i_{90} = i_a \sin\varphi \quad (3)$$

The explanation for (2) and (3) is based on two factors:

(1) The electromotive forces behind the Potier reactance ( $e_p$ ) have approximately the same values in the reactive load regime,  $i_{a,90} = i_{an} \cdot \sin\varphi_n$ , and in the nominal generator regime, i.e.  $e_{p90} \approx e_{p,n} = 0C$  (Fig. 4), which makes the corresponding main turbogenerator magnetic fluxes to be also equivalent.

(2) The corresponding components of the direct-axis leakage flux of the excitation coil (of the rotor) are also equivalent as they, just as the components of the direct-axis magnetic leakage of the stator coil, depend almost exclusively on the reactive load.

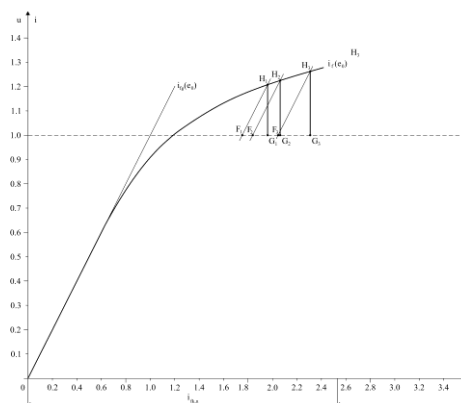


Figure 2. Potier reactance values,  $X_{P(A1)} < X_{P(A2)} < X_{P(A3)}$  for three different armature currents ( $i_{a1(C1)} > i_{a2(C2)} > i_{a3(C3)}$ ) and corresponding points  $A_1, A_2, A_3$  (from Fig. 1)

From (1) and (2) it follows that the corresponding direct axis fluxes and magnetic saturation on the stator and rotor parts are approximately equivalent in both cases. For that reason the Potier reactance values for the rated regime and the reactive load regime with  $i_{a,90} = i_{an} \cdot \sin\varphi_n$ , i.e.  $x_{p,n} \approx x_{p,90n}$  (Fig. 4) are also approximately equivalent. The above proofs are sufficient for the conclusion that the Potier reactance values for drawing the given voltage value, depend almost exclusively on the reactive load component ( $i_{a,90} = i_{an} \cdot \sin\varphi_n$ ).

The above rule is tested on the example of a GTHW 360 (360 MW) turbogenerator by comparing - the measured values of the generator excitation current ( $I_{F, meas}$ ) for the regimes around the rated regime:

$P_G \approx P_{Gn}$  and  $Q_G \approx Q_{Gn}$ , and  
 - the calculated values ( $I_{F, calc}$ ) based on the Potier  
 reactance values ( $x_{P,90}$ ) determined for  $i_{a,90} \approx i_{an} \cdot \sin\varphi_n$ ,  
 $Q_{90} = Q_{Gn}$ .

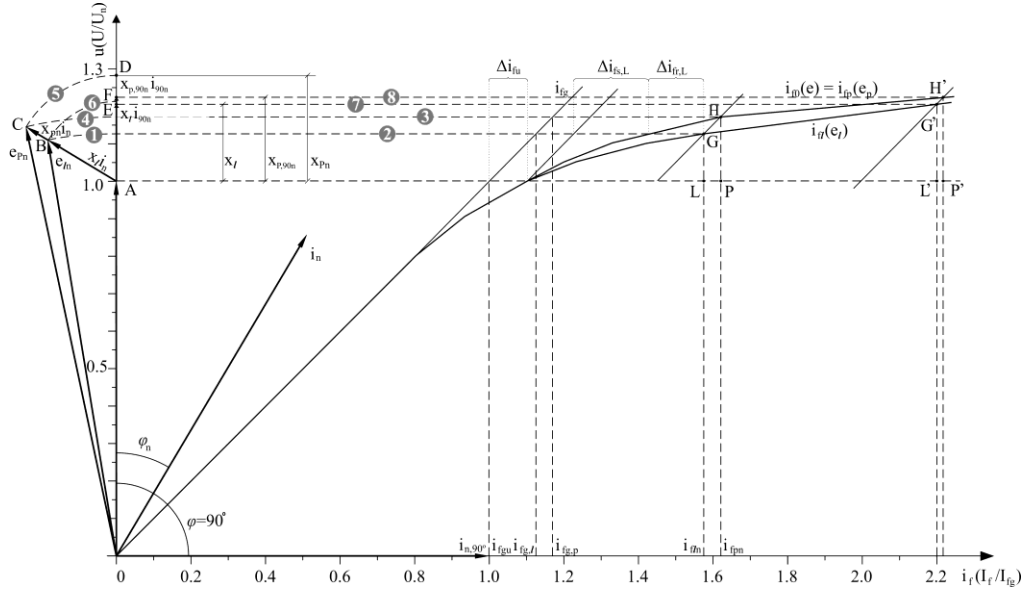


Figure 3. Vector diagrams of the electromotive forces behind the Potier reactance ( $e_p$ ) and behind the leakage reactance ( $e_l$ ), and procedure to determine the Potier reactance ( $X_p$ ):

$X_{pn}$  for the rated generator regime ( $u = u_n$ ,  $i = i_n$  and  $\varphi = \varphi_n$ ) from 1–6; and

$X_{p,90n}$  by the reactive load test with rated current  $i_{90} = i_n$  ( $u = u_n$ ,  $i_{90} = i_n$  and  $\varphi = 90^\circ$ ) from 7–8

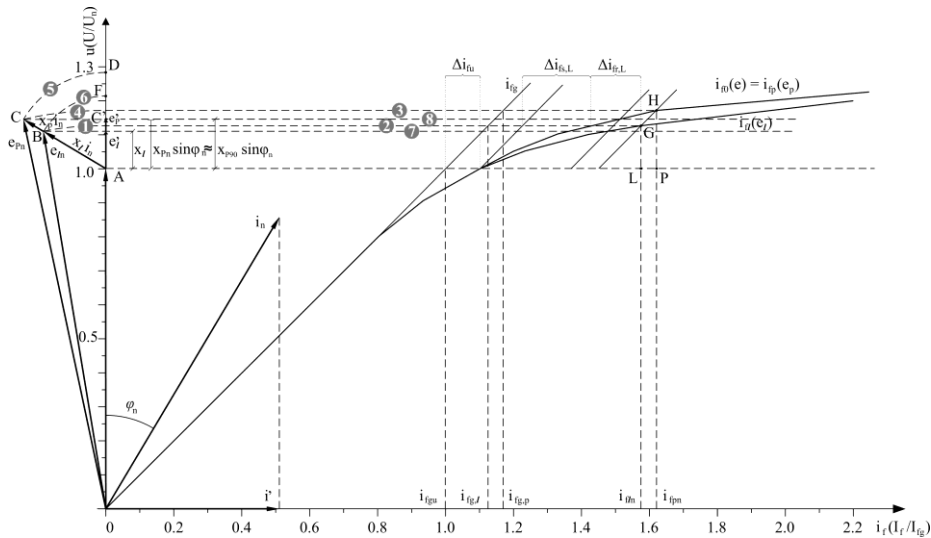
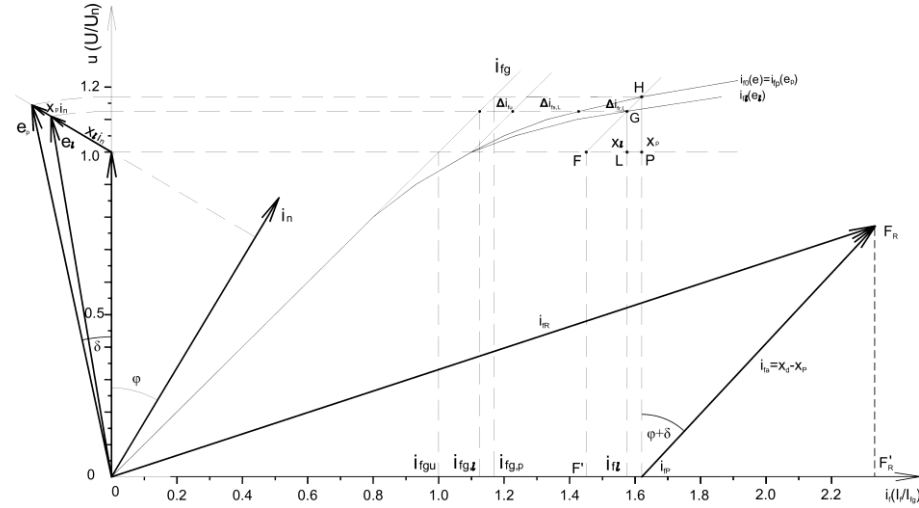


Figure 4. Vector diagrams of the electromotive forces,  $e_p$  and  $e_l$ , and procedure to determine the Potier reactance:

$x_{p,n}$  for the rated generator regime ( $u = u_n$ ,  $i = i_n$  and  $\varphi = \varphi_n$ ) from 1–6, and

$x_{p,90n}$  by the reactive load test with armature current  $i_{90} = i_{an} \cdot \sin\varphi_n$  ( $u = u_n$ ,  $i_{90} = i_{an} \cdot \sin\varphi_n$  and  $\varphi = 90^\circ$ ) from 7–8


 Figure 5. Vector diagrams of the electromotive forces,  $e_p$  and  $e_r$ , and vector diagram to determine the excitation current values

#### 4 AN EXAMPLE OF APPLICATION AND TESTING OF A RATED GENERATOR REGIME

As an example, the Potier reactance values,  $x_{p,90}$ , were determined from the data of the reactive load test and the given generator no-load characteristics,  $I_{F0}(U_0)$ . The results obtained for the Potier reactance are given in Table 1, for three turbogenerator reactive load values:

1. For values  $Q_{G1} = Q_{Gmax} > Q_{GN}$ , corresponding to the rated excitation current  $I_f = I_{fN}$ ;
2. For values  $Q_{G2} = Q_{GN}$ , at voltage  $U_{G2} = U_G$  for  $Q_{G2} = Q_N$ ; and
3. For values  $Q_{G3} = (Q_{Gmax} + Q_{GN})/2$ , at voltage  $U_{G3} = U_G$  for  $Q_{G3}$ .

It should be noted that the reactive load test is conducted with the generator connected to a large-capacity power system for which a constant voltage  $V_{EES}$  may be assumed (i.e. infinite bus), and that the generator voltage ( $V_G$ ) only changes due to the changes in the voltage level at the block transformer when there is a change in the reactive loads. This enables the Potier reactance change to take place in real regimes at a change in the reactive loads, as it is only the change that leads to perceptible voltage changes in the synchronous generator connected to an infinite bus.

The Potier reactance values,  $x_p$ , are determined by the open-circuit saturation curves and from the reactive load test with armature current  $i_{a,90} = i_{an} \sin \varphi_n$  and  $U = U_n$  (Fig. 5). From Fig. 5, equation (4) is obtained for the excitation current component ( $\Delta i_{fr}$ ) due to the rotor additional saturation in the load regime

$$\Delta i_{fr,L} = i_f - i_{fl} - (x_d - x_l) i_{a90} \quad (4)$$

When  $x_l = x_p$ , then  $\Delta i_{fr} = 0$  (Fig. 5), i.e.

$$i_f - i_{fl} - (x_d - x_l) i_{a90} = 0 \quad (5)$$

Using equation (5), all procedures for determining the Potier reactance ( $x_p$ ) are performed by computer (in an Excel program), and the open-circuit saturation curves  $i_{f0}(e_0)$  are expressed analytically. With this the procedure is simplified and more precise. The required Potier reactance values ( $X_p$ ) determined by equation (5) are given in Table 1. As seen from the results in Table 1, the Potier reactance value significantly increases as the reactive load decreases (by up to 20%).

The author's thesis that the value of the Potier reactance (practically) does not change with the active generator power when the reactive load value remains constant was verified on two regimes around the rated current ( $P_G \approx P_{Gn}$  and  $Q_G \approx Q_{Gn}$ ), i.e. by comparing:

- measured values  $I_{f, meas}$  (Table 2, type 1a and 2a), and
- calculated values  $I_{f, calc}$ , on the basis of the Potier reactance values ( $x_{p,90}$ ) determined by the reactive load test for  $Q_{G,90} = Q_{Gn}$ .

Table 1: Data from the reactive load test of the GTHW 360Turbogenerator and results of the Potier reactance ( $x_p$ ) calculation  $X_s = X_d$

$X_s = X_d$ p.u.	P MW	Q Mvar	$U_G$ kV	$X_p$ p.u.	$I_F$ A	$E_{fr}$ %
Regime 1						
1a.Meas	321	216	23.0	/	2502	
1b.Calc.	321	216	23.0	0.273	2480	-0.88
Regime 1						
1a.Meas	321	231	23.3	/	2589	
1b.Calc.	321	216	23.3	0.273	2569	-0.77

$$i_f = \sqrt{[i_{fp} + (x_d - x_p)(s/u)(\sin \varphi \cos \delta + \cos \varphi \sin \delta)]^2 + [(x_d - x_p) \cdot (\cos \varphi \cos \delta - \sin \varphi \sin \delta)]^2} \quad (6)$$

Table 2: Measured (1a and 2a) and calculated (1b and 2b) values of the excitation currents for generator voltages ( $U_{Gn}=23$  kV) and currents around the rated values

$X_s=X_d$ p.u.	P MW	Q Mvar	$U_G$ kV	$U_G/U_{Gn}$ p.u.	$I_F$ A	$X_p$ p.u.
Regime with the maximally permitted reactive power ( $Q_{G,max}$ ), for $\text{Cos}\varphi\approx 0$ ( $Q_{G,max}\approx 1.3 Q_{Gn}$ )						
2.535	33.1	296.0	23.77	1.080	2549.	0.258
Regime with rated reactive power ( $Q_{Gn}$ ), for $\text{Cos}\varphi\approx 0$						
2.535	33.5	216.0	23.22	1.055	2048.	0.273
Regime with reactive power $Q_G=(Q_{Gn}+ Q_{G,max})/2$ , for $\text{Cos}\varphi\approx 0$						
2.535	32.0	256.0	23.66	1.075	2296.	0.265
Regime with reactive power $Q_G=0.617Q_{Gn}$ , for $\text{Cos}\varphi\approx 0$						
2.535	33.5	133.4	22.61	1.028	1533.	0.287

The values of the excitation current ( $i_f$ ), per unit, for the above determined values of the Potier reactance ( $x_p,90$ ) can be calculated using expression (6) derived from a right triangle OFRFR' (Fig. 6). Values  $\cos\delta$ ,  $\sin\delta$  and  $i_fP$  are calculated for the parameters of given regimes  $s = S/S_n = 1$ ,  $p = P_n/S_n = \cos\varphi$ ,  $q = Q/S_n = \sin\varphi$  and  $u = U/U_n = 1$ . Values  $i_{f0}(e_p)$  are determined by the observed dependence  $i_{f0}(e)$ , for  $e = e_p$ . As the stated dependence  $i_{f0}(e)$  is given in an analytical form, the complete procedure for calculating the value of  $i_f$  (or  $i_{f,n}$ ) is automated and can be managed by a PC.

The calculated excitation current values of the generator  $I_F$  differ, in turn, by (-0.88%) and (-0.77%), which is within the accuracy limits of the measured excitation current ( $I_F$ ) values. The accuracy is expected to be even higher in the region of larger reactive power values, as the corresponding active power is smaller and the regime therefore differs less from the referent a reactive load regimes for which the Potier reactance values are determined.

## 5 CONCLUSION

Based on an extensive research, the author shows an important conclusion that the Potier reactance values, for a given voltage value, almost exclusively depend on the reactive load ( $i_{aQ} = i_a \cdot \sin\varphi$ ) component. This thesis was proven:

- firstly, by a general qualitative analysis, and
- then verified on two regimes around the rated value ( $P_G \approx P_{Gn}$  and  $Q_G \approx Q_{Gn}$ ),

i.e. by comparing the measured and calculated field currents on the analyzed 360 MW turbogenerator. The Potier reactance values ( $x_p$ ) were determined by a reactive load test for  $Q_{G,90} \approx Q_{Gn}$ .

On the basis of these results, the author proposes the Potier reactance values to be determined with a reactive load test (overexcitation) for the rated voltage and armature current value  $i_{a,90} = i_{an} \cdot \sin\varphi_n$ , and for some characteristic values which would be convenient for the

determining the turbogenerator capability curves (P-Q curve). Changing the corresponding IEC 34-4 standard [9] in the part on the determination of the Potier reactance is also proposed.

## REFERENCES

- [1] A.M. El-Serafi, J. Wu, "A New Method for Determining the Armature Leakage Reactance of Synchronous Machines", *IEEE Trans. on En. Conv.*, Vol. 6, No. 1, March 1991, pp. 120-125.
- [2] A.B.J. Reece, A. Pramanik, "Calculation of the End Region Field of A.C. Machines", *Proc. IEE*, Vol. 112, 1965, pp. 1355-1368.
- [3] R.G. Slemmon, "Analytic Models for Saturated Synchronous Machines", *IEEE Trans. on Power Apparatus and Syst.*, Vol. PAS-90, 1971, pp. 409-417.
- [4] E.A. Abdel-Halim, C.D. Manning, "Modelling Saturation of Laminated Salient-Pole Synchronous Machines", *Proc. IEE*, Vol. 134, Pt. B, pp. 215-223.
- [5] J.O. Ojo. and T.A. Lipo, "An Improved Model for Saturated Salient Pole Synchronous Motors", *IEEE Trans. on Energy Conv.*, Vol. EC-4, 1989, pp. 135-142.
- [6] M. Liwshitz-Garik, C.C. Whipple, *A-C Machines*, D. Van Nostrand Company Inc., New York, Toronto, London, 1964.
- [7] J.C. Flores, G.W. Buckley, G. McPherson Jr., "The Effects of Saturation on the Armature Leakage Reactance of Large Synchronous Machines", *IEEE Tran on Pow App. and Sys*, Vol. PAS-103, pp. 593-600.
- [8] R. Bourne, *Electrical Rotating Machine Testing*, Iliffe Books Ltd, London, 1969.
- [9] *IEC 34-4/2008*, Part 4: Methods for determining synchronous machine quantities from tests.
- [10] *Determining of Generator Capability Curves by New Method for Determination of Potier reactance curves (P-Q curve) for generators B1 and B2 in Thermal Power Plan Kostolac B*, Technical Report, Electr. Eng. Institute - Nikola Tesla, Belgrade, 2009, pp. 59 (in Serbian).
- [11] M.M. Kostić, "A New Method for Determining the Potier Reactance of Synchronous Turbogenerators", *Elektroprivreda*, No. 4, 2009, pp. 59-68 (in Serbian).
- [12] M.M. Kostic, B. Kostić, M. Ivanović, "Construction Generator Capable Curves by of New Method for Determining of Potier Reactance", *International Conf on Power Plants*, 2010, Vrnjačka Banja, Serbia.
- [13] I. Boldea, *Synchronous Generators - The Electric Generator Handbook*, 2006, pp. 512, Taylor & Francis Group, Boca Raton, New York, London, 2006.

**Miloje Kostic** was born in Bioska, Serbia, in 1950. He received his B.Sc. and M.Sc. degrees in electrical engineering from the University of Belgrade, Serbia, in 1974 and 1983, respectively, and his Ph.D. degree from the University of Kragujevac, Serbia, in 1990.

From 1974 to 1991 he worked at the Industrial plant "Prvi partizan", Uzice, Serbia. In 1991 he joined the "Nikola Tesla" Electrical Institute, Belgrade, where he is currently Senior Consultant.

His fields of interest include Theoretical Electrical Engineering, Induction Heating, Industrial Energy and Electrical Machines. He has written some 140 technical papers published in journals and conference proceedings, four books and is the owner of five patents.